Sustainability in Environment
ISSN 2470-637X (Print) ISSN 2470-6388 (Online)
Vol. 11, No. 2, 2026
www.scholink.org/ojs/index.php/se

Original Paper

Analysis of the Evolution of Landscape Pattern of Land Use：Taking Shibing Karst and Libo-Huanjiang Karst as an Example

Qian Zhai[1,2], Kangning Xiong[1,2,*], Jiacheng Lan[1,2], Yating Mu[1,2], & Qingqing Xie[1,2]

[1] School of Karst Science, Guizhou Normal University, Guiyang, China

[2] State Engineering Technology Institute for Karst Desertification Control,Guiyang, China

[*] Corresponding Author

Received: February 01, 2026 Accepted: March 12, 2026 Online Published: March 23, 2026

doi:10.22158/se.v12n1p76 URL: http://dx.doi.org/10.22158/se.v12n1p76

Abstract

This study takes the Shibing Karst and Libo-Huanjiang Karst as research objects, based on land use data from 2000 to 2020, combined with landscape pattern index, land use dynamic attitude, and transfer matrix method, to analyze the transformation characteristics and spatiotemporal evolution patterns of landscape patterns in these two karst regions. The results show that forest land and farmland are the dominant landscape types in the two study areas. Spatially, the high-value areas of aggregation and connectivity indices in the Shibing Karst are concentrated in the central region, while the high-value areas of diversity and shape complexity indices are located in the northern and southeastern regions. In the Libo-Huanjiang Karst, the high-value areas of aggregation and connectivity indices are distributed in the eastern region, and the low-value areas are located in the central region, which gradually shifted to the central region after 2010. The high-value areas of diversity indices are concentrated in the central, western, and northern regions. This study reveals the spatiotemporal evolution characteristics of landscape patterns in typical karst World Heritage sites in southern China from 2000 to 2020, providing a scientific basis for optimizing the landscape patterns of karst World Heritage.

Keywords

landscape pattern, land use s, spatiotemporal evolution, world heritage karst sites

1. Introduction

Landscape patterns, formed through spatial interactions of natural or human-made landscape elements of varying sizes and shapes, constitute a vital component of landscape ecology research (Turner, 2005). As a key driver of landscape pattern evolution, land use transformation directly alters landscape

structures, which in turn impacts ecosystem components, structures, and processes, ultimately leading to dynamic changes in ecosystem services (Su, Xiao, Jiang, & Zhang, 2012; Fu, Wang, Su, & Forsius, 2013).

The UNESCO World Heritage Committee and Chinese government have explicitly stated that World Heritage, as shared cultural and natural treasures of humanity, their protection and rational utilization are directly linked to ecological security maintenance, regional sustainable development, and social well-being improvement. However, while the World Heritage is prioritized for ecological protection, they also face significant threats from natural factors and anthropogenic pressures (Allan, Venter, Maxwell, Bertzky, Jones, Shi, Watson, 2017; Fei, Xiong, Fei, Zhang, & Zhang, 2023; Luo, Wang, Chen, Wang, & Guo, 2024). These threats inevitably alter the structure and processes of heritage ecosystems, ultimately leading to the degradation of ecosystem service functions (Xiong, Chen, Zhang, Gu, & Zhang, 2023). Numerous studies have demonstrated that changes in ecosystem services caused by Land Use/Cover Change (LUCC) are extensive and profound (Wang, Dai, Ge, Zhang, & Yu, 2021), exerting significant impacts on biodiversity (Yan, & Li, 2023), regulating services (Liu, Hou, Li, Song, & Wang, 2020). Therefore, clarifying the spatiotemporal variations in land use and different landscape pattern indices can provide basic data and theoretical support for scientifically identifying key ecological protection areas in heritage sites, optimizing landscape pattern configuration, and formulating targeted ecological protection and management strategies. This further contributes to safeguarding the Outstanding Universal Value and ecosystem integrity of Karst World Heritage Sites, and realizing the coordinated advancement of ecological protection and sustainable development in these sites.

Karst landscapes worldwide are primarily concentrated in three major regions: the Mediterranean coast, eastern North America, and southern China (Sweeting, 1986; Ford & Williams, 2007). Among these, the karst area in southern China exceeds 550,000 km², representing the most typical, complex, and landscape-diverse tropical-subtropical karst region globally. It is also the largest and most contiguous karst ecologically fragile zone worldwide (Yang, 1990). Consequently, the ecosystems of karst World Natural Heritage sites in southern China are more vulnerable compared to other World Natural Heritage sites (Xiong, Li, & Wang, 2012). World Heritage (WH) sites are recognized as the most unique representatives on Earth due to their outstanding universal value (OUV) (Kenterelidou, & Galatsopoulou, 2021). Karst resources and environments exhibit distinct characteristics of fragility, sensitivity, and vulnerability, with generally low natural regeneration capacity [17]. Despite these challenges, the region has nurtured seven unique World Natural Heritage sites, with Shabing and Libo-Huanjiang Karst being outstanding representatives.

Therefore, aiming at the key scientific problem of the lack of systematic and scientific research on the landscape patterns of Karst World Heritage Sites, this study selected Shibing Karst and Libo-Huanjiang Karst as typical study areas—these two sites can represent the overall conservation value and attribute characteristics of karst landscapes in southern China. We analyzed the characteristics of land use changes in Karst World Heritage Sites from 2000 to 2020 and adopted the moving window method to

explore the spatiotemporal evolution laws of landscape patterns.

2. Materials and Methods

2.1 Study Areas

The Shibing Karst is located in the eastern part of Guizhou Province in southwest China (Figure 1), in the slope transition zone (N27°05′49″~N27°13′59″, E108°01′34″~E108°09′32″) from the eastern edge of the the Yunnan-Guizhou Plateau to the low mountains and hills in western Hunan, with an average altitude of 912 m, in the subtropical monsoon humid climate zone, with an average annual temperature of about 16°C, an average annual rainfall of 1220 mm, dense vegetation coverage, and a forest coverage rate of about 93.95% (Liu, Wang, Xiong, Gong, Chen, Yang, Xiao, & Bai, 2024). The formation lithology is mainly pure, dense, thin and fine-grained dolomite, and the rock is generally broken. The soil type is mainly thin lime soil formed by dolomite weathering (Bai, Xiong, Chen, & Liu, 2024). The karst of Shibing Cone shaped Peak Cluster Canyon demonstrates the unique development and evolution process of cone shaped peak cluster canyon on the basis of dolomite in humid tropical subtropical environment, which is unique in the world karst and fills the gap of dolomite in the southern karst world heritage.

The Libo-Huanjiang Karst is located at the junction of Libo County in Qiannan Prefecture, Guizhou Province and Huanjiang County in Hechi City, Guangxi Zhuang Autonomous Region (E107°58′30″~107°59′40″, N25°09′27″~25°13′15″), mainly including the Daqikong and Xiaoqikong scenic spots in Maolan National Nature Reserve and Zhangjiang National Scenic Area, as well as the Mulun National Nature Reserve in Guangxi. The Libo-Huanjiang Karst is located in the subtropical monsoon climate zone, with an average annual temperature of 15.3 ℃, an average annual rainfall of 1752mm, and an average altitude of 747m (Tian, 2008). The soil is mainly composed of neutral to slightly alkaline limestone soil, with black limestone soil being the most common. The sedimentary rock thickness in the study area is 8600m, and the lithology includes limestone, dolomite, and dolomitic limestone. Under unique geographical conditions, the Libo-Huanjiang Karst has developed a typical subtropical cone-shaped karst landform, preserving the most complete and largest native evergreen deciduous broad-leaved mixed forest ecosystem in the same latitude region of the world (Zhang, 2025).

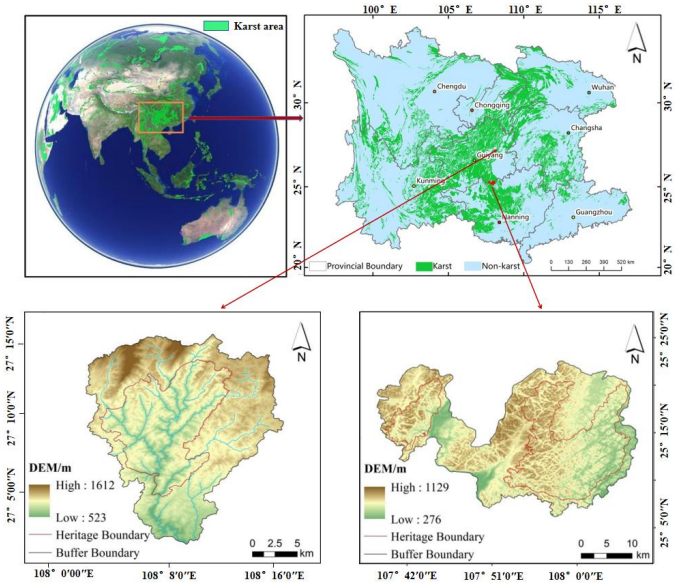

Figure 1. Distribution of the two World Heritage Sites in South China. The Left Side Shows the Shibing Karst. The Right Side Shows the Libo-Huanjiang Karst

2.2 Data Sources

In this study, remote sensing imagery of the two research regions from 2000 to 2020 was collected first, using ENVI 5.6 and ArcGIS 10.8 software were utilized to complete sequential preprocessing operations for the remote sensing images, which included radiometric calibration, atmospheric correction and image alignment. The land use classification system was formulated according to the criterion of "Current Land Use Classification" (GB/T21010-2017), and adjusted by considering the actual land cover conditions of the study area; accordingly, the land use types were categorized into farmland, forest, shrub forest, grassland, water body and construction land.

2.3 Method

2.3.1 Dynamic Degree of Land Use

As a key evaluation index for land use change, land use dynamic degree can effectively measure the quantitative variation of land use type quantity in the study area. In this study, we selected the single land use dynamic degree and comprehensive land use dynamic degree (Chen, Tong, & Guo, 1998) for the analysis of land use change in the two World Heritage sites, and the relevant calculation formulas are shown below:

$$K=\frac{U_b-U_a}{U_a}\times\frac{1}{T}\times 100\% \quad (1)$$

In the formula, Krepresents the dynamic attitude of a specific land use type during the study period; U_a、U_b are the quantities of that specific land use type at the beginning and end of the study period, respectively; $T$when $T$the period is set to one year, $K$the value is the annual dynamic attitude of that specific land use type in the study area.

$$LC=\frac{\sum_{i=1}^{n}\Delta LU_{ij}}{2\sum_{i=1}^{n}LU_i}\times\frac{1}{T}\times 100\% \quad (2)$$

In this formula, i and j represent land use types; LU_i denotes the area of land use type i in the initial study period; ΔLU_{ij} represents the area converted from land use type i to land use type j during the study period; T is the duration of the study period, which in this paper is also measured in years, thus expressed as the annual comprehensive land use dynamic.

2.3.2 Land Use Transfer Matrix

The landscape type conversion matrix can explain the changes that occur between various landscape types, highlight the structural characteristics of the terrain, and the mutual changes and directions that occur between various landscape types [23-24]. The calculation formula is as follows:

$$S_{ij}=\begin{bmatrix} S_{11} & S_{12} & \cdots & S_{1n} \\ S_{21} & S_{22} & \cdots & S_{2n} \\ \vdots & \vdots & & \vdots \\ S_{n1} & S_{n2} & \cdots & S_{nn} \end{bmatrix} \quad (3)$$

In the formula, S_{ij} represents the area of land use type j converted to land use type i during the study period; i represents the original land use type before conversion; j represents the land use type after conversion; represents the number of land use types.

2.3.3 Landscape Pattern Index

This study followed the principles of low redundancy between indices, being able to characterize ecological status, and having a concise and easy to understand calculation logic for screening. Ultimately, seven indicators were selected, including the maximum patch index (LPI), patch aggregation index (COHESION), average patch area (AREA_MN), average proximity index (CONTIG_MN), average shape index (SHAPE_MN), Shannon diversity index (SHDI), and Shannon evenness index (SHEI) (Table 1). Fragstats 4.2 was used to calculate seven landscape form indices, and raster images of the seven landscape pattern indices were obtained.

Table 1. Selection of Landscape Pattern Indices and Calculation Methods

Variables	Abbreviation	Formula
Largest Patch Index	LPI	$LPI=\frac{max_{k=1}^{n_p}(a_k)}{A_L}\times 100\%$
Shannon's Diversity Index	SHDI	$SHDI=-\sum_{i=1}^{m}P_i ln(P_i)$

Shannon's Evenness Index	SHEI	$SHEI=\frac{-\sum_{i=1}^{m} p_i ln(p_i)}{ln(m)}$
Patch Cohesion Index	COHESION	$COHESION=1-\frac{\sum_{i-1}^{n} a_i}{\sum_{i-1}^{n} a_i \sqrt{p_i}} \times (1-\frac{\sum_{i-1}^{n} a_i^2}{(\sum_{i-1}^{n} a_i)^2})^{-1}$
Mean Patch Contiguity	CONTIG_MN	$CONTIG\_MN=\frac{1}{n} \times \frac{[\frac{\sum_{r=1}^{z} C_{ijr}}{a_{ij}}]-1}{V-1}$
Mean Shape Index	SHAPE_MN	$SHAPE\_MN=\frac{1}{n} \times \frac{0.25P_{ij}}{\sqrt{a_{ij}}}$
Mean Patch Area	AREA_MN	$AREA\_MN=\frac{\sum_{i=1}^{n} a_{ij}}{n_i}(\frac{1}{10000})$

3. Results

3.1 General Characteristics of Landscape Transition

3.1.1 Characteristics of Land Use Change

The results showed that the landscape types of Shibing Karst and Libo-Huanjiang Karst were mainly forest land and cultivated land (Figure 2), with forest land accounting for over 83% and 88% respectively, both of which were dominant landscape types and concentrated in the core area. Cultivated land accounted for over 8.6% and 5% respectively, mainly distributed in the buffer zone, and other land use types accounted for relatively low proportions. As of 2020, the cultivated land in the Shibing Karst has grown the most significantly, increasing by 16.49 km^2, while the forest area has decreased significantly, decreasing by 15.99 km^2, and the water area has remained stable (Table2). The forest land in the Libo-Huanjiang Karst area has grown significantly, with an increase of 8.6 km^2; The reduction in shrub area was relatively significant, with a decrease of 16.75 km^2 (Table3).

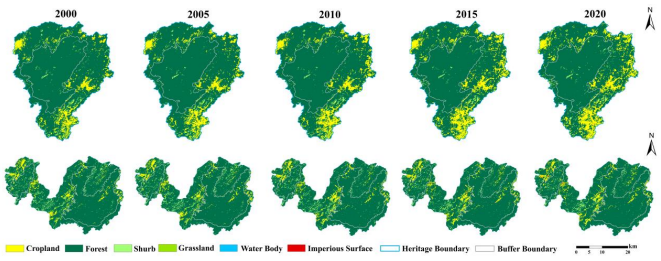

Figure 2. Spatial Distribution of Landscape Types in Shibing Karst and Libo-Huanjiang Karst

Table 2. Land Use Change in Shibing Karst from 2000-2020

Land use types	Cropland		Forest		Shurb		Grassland		Water Body		Imperious Surface	
Year	Area (km²)	Proportion (%)	Area (km²)	Proportion (%)	Area (km²)	Proportion (%)	Area (km²)	Proportion (%)	Area (km²)	Proportion (%)	Area (km²)	Proportion (%)
2000	24.37	8.60	252.27	89.05	6.58	2.32	0.05	0.02	0.03	0.01	0.01	0.00
2005	27.51	9.71	249.76	88.16	5.92	2.09	0.06	0.02	0.03	0.01	0.02	0.01
2010	29.83	10.53	247.69	87.43	5.63	1.99	0.08	0.03	0.03	0.01	0.04	0.02
2015	37.96	13.40	240.28	84.81	4.92	1.74	0.05	0.02	0.03	0.01	0.08	0.03
2020	40.86	14.42	236.28	83.40	5.33	1.88	0.68	0.24	0.03	0.01	0.12	0.04

Table 3. Land Use change in Libo-Huanjiang Karst from 2000-2020

Land use types	Cropland		Forest		Shurb		Grassland		Water Body		Imperious Surface	
Year	Area (km²)	Proportion (%)	Area (km²)	Proportion (%)	Area (km²)	Proportion (%)	Area (km²)	Proportion (%)	Area (km²)	Proportion (%)	Area (km²)	Proportion (%)
2000	41.90	5.14	723.80	88.77	48.79	5.98	0.53	0.07	0.28	0.03	0.03	0.00
2005	58.03	7.12	706.14	86.61	50.40	6.18	0.30	0.04	0.39	0.05	0.07	0.01
2010	44.22	5.42	728.47	89.35	41.93	5.14	0.26	0.03	0.32	0.04	0.14	0.02
2015	49.58	6.08	729.48	89.47	35.22	4.32	0.31	0.04	0.36	0.04	0.38	0.05
2020	49.19	6.03	732.40	89.83	32.04	3.93	0.25	0.03	0.44	0.05	1.00	0.12

3.1.2 Dynamic Degree of Land Use

The results showed that the dynamic degree of forest land in the Shibing Karst was negative, with the highest dynamic degree of cultivated land being 0.055% from 2010 to 2015, the dynamic degree of construction land reaching 0.215% from 2005 to 2010, and the dynamic degree of shrubs changing from negative to positive from 2015 to 2020. The water area was basically stable, and the dynamic degree of comprehensive land use in all four periods was below 50%; The dynamic degree of construction land in Libo-Huanjiang Karst was the highest from 2010 to 2015, at 0.360%; The dynamic degree of water body from 2000 to 2005 was the highest, at 0.083%, while the dynamic degree of forest land was the lowest in the four periods, and the comprehensive land use in all four periods did not exceed 55% (Table 4).

Table 4. Land Use Dynamics in Shibing karst and Libo-Huanjiang Karst from 2000-2020

Land use Dynamics	Shibing karst				Libo-Huanjiang karst			
	land use dynamics(%)							
cropland	0.026	0.017	0.055	0.015	0.077	-0.048	0.024	-0.002
forest	-0.002	-0.002	-0.006	-0.003	-0.005	0.006	0	0.001
shurb	-0.020	-0.010	-0.025	0.017	0.007	-0.034	-0.032	-0.018
grassland	0.046	0.066	-0.082	2.808	-0.088	-0.028	0.042	-0.037
Water Body	0.000	-0.007	0.007	-0.007	0.083	-0.034	0.023	0.046
Imperious Surface	0.129	0.215	0.154	0.120	0.211	0.185	0.360	0.328
Integrated Land Use Dynamics(%)	0.28	0.29	0.48	0.37	0.46	0.51	0.43	0.38

3.1.3 Land Use Transfer Matrix

According to the transition matrix and chord diagram, it can be seen that the land use changes in the Shibing Karst were mainly dominated by the conversion between cultivated land and forest land in the four time periods, with continuous conversion between the two during the periods of 2000-2005 and 2005-2010; From 2010 to 2015, the area of cultivated land transferred increased to 9.60 km², and the area of forest land transferred was 9.75 km², mainly converted into cultivated land and shrubs; The area of cultivated land transferred from 2015 to 2020 is still dominated by the transfer of forest land. The conversion of grassland, shrubs, and construction land is showing an increasing trend. The land use changes in the four periods of Libo-Huanjiang Karst are concentrated between forest land, cultivated land, and shrubs. Forest land is mainly converted into cultivated land and shrubs, with the highest conversion during the period of 2000-2005. The areas converted into cultivated land and shrubs were 13.62km²and 11.99km², respectively. Shrubs were mainly converted into forest land and cultivated land,

with a total conversion of 17.572 km from 2005 to 2010 (Figure 3).

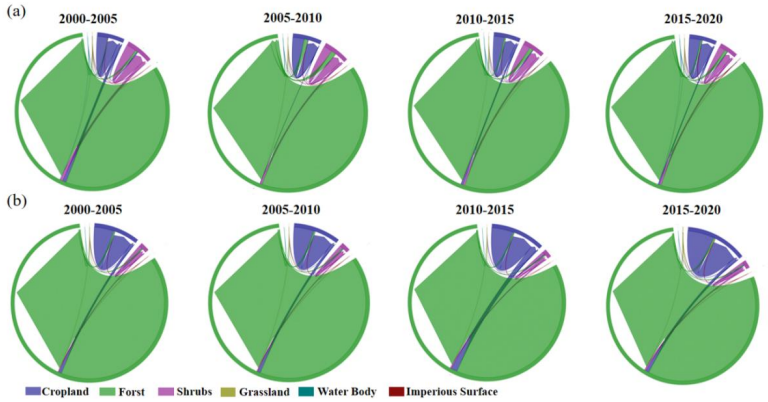

Figure 3. Matrix Chord Diagram of Landscape Type Yransition. a presents the matrix chord diagram of landscape type transition in Shibing Karst; b presents the Matrix chord diagram of landscape type transition in Libo-Huanjiang Karst

3.1.4 Spatial and Temporal Changes in Landscape Pattern Index

From the perspective of temporal changes, there has been a slight increase in SHDI and SHEI in the Shibing Karst; The LPI and COHSION values remain above 80, while the AREA_MN values are between 13-15.60. CONTIG_MN and SHAPE_MN show an upward trend. The SHDI and SHEI of the Libo-huanjiang Karst showed a slight increase in 2000 but gradually decreased in 2010. The COHESION value remained above 99, while AREA_MN and CONTIG_MN showed slight fluctuations with an increase in the final values. LPI exceeded 88 except in 2005, and SHAPE_MN showed a slight downward trend (Figure 4).

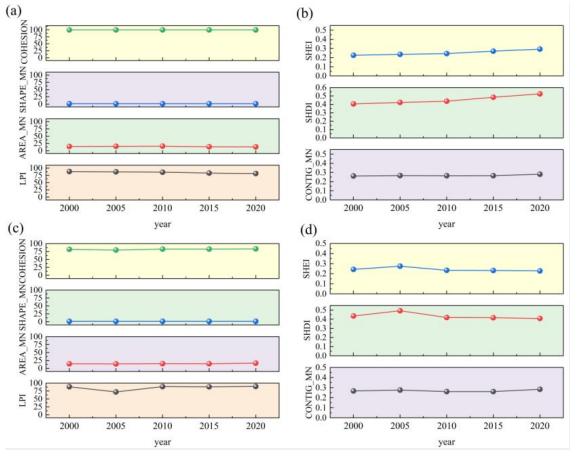

Figure 4. Landscape pattern indices at the landscape level for karst World Heritage Sites from 2000 to 2020. a,b represent Shibing Karst ;c,d represent Libo-Huanjiang Karst

From a spatial distribution perspective, the high-value areas of Shibing Karst CONHESION,

AREA_MN, CONTIG_MN, and LPI are concentrated in the central part of the heritage site, while the low to medium value areas are mainly distributed in the northern and southeastern parts. The low value areas of SHAPE_MN, SHDI, and SHEI are concentrated in the central part of the heritage site. The high value areas of SHAPE_MN, SHDI, and SHEI are mainly distributed in the north and southeast. From 2015 to 2020, the high value areas of SHAPE_MN gradually transformed into low value areas, and from 2010 to 2020, the high value areas of SHDI gradually transformed into low value areas (Figure 5). From 2000 to 2020, the high-value areas of AREA_MN, COHESION, and CONTIG_MN in the Libo-Huanjiang Karst were located in the east, the median areas were distributed in the west and north, and the low value areas were concentrated in the central region; The high value area of LPI is mainly located in the east, while the low value area is located in the middle. After 2010, the low value area gradually transformed into the median area. The low value areas of SHAPE_MN, SHDI, and SHEI are mainly distributed in the east, while the medium high value areas are concentrated in the central, western, and northern regions. Among them, SHAPE_MN gradually transformed from the high value area to the median area in 2020 (Figure 6).

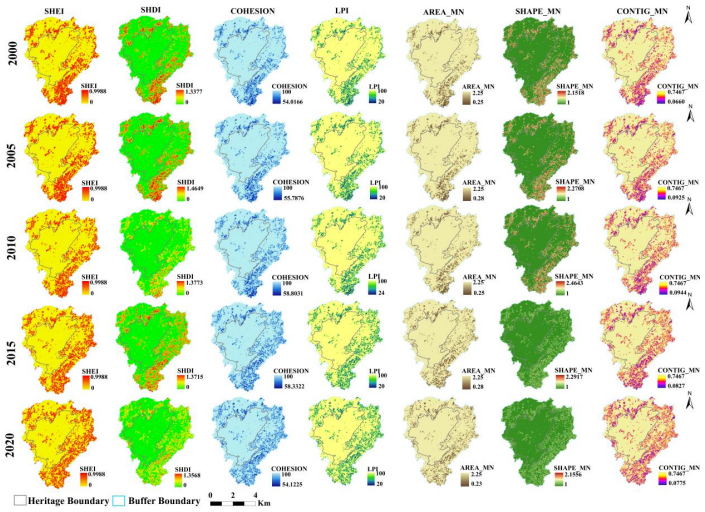

Figure 5. Spatial Distribution Characteristics of Landscape Pattern in Shibing Karst

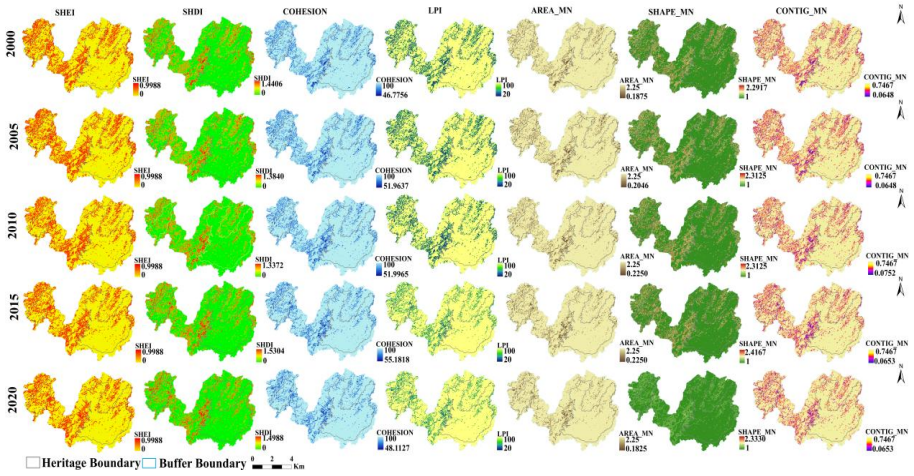

Figure 6. Spatial Distribution Characteristics of Landscape Pattern in Libo-Huanjiang Karst

4. Discussion

The results indicate that the KWH sites generally have higher regulatory service functions than buffer zones, a result mainly attributed to the strict protection of core areas, while buffer zones are often threatened by human activities such as agricultural development and tourism (Chen, Cheng, Xiong, Rong, & Zhang, 2024). Our research also found that from 2000 to 2020, CS in Shibing Karst and WC at two sites showed a slight downward trend. However, under the background of rising threats and decreasing support, such reports are not only prevalent in China but also worldwide (Osipova et al., 2017). Currently, KWH sites are facing rapid degradation of ecosystem services, a phenomenon that may be closely related to the continuous increase in human activity intensity. For example, we found that between 2000 and 2020, the areas of cultivated land and construction land at two KWH sample sites increased. These results may indicate that ecological protection and conservation were not well implemented at the KWH sites studied here, and the increase in cultivated land area also reflects this (Chen, Cheng, Xiong, Rong, & Zhang, 2024). Extensive evidence demonstrates that forest land reduces soil organic carbon loss through microbial community regulation and mitigates soil erosion risks by enhancing aggregate stability (Lan, Wang, Wang, Qi, Long, & Huang, 2022). Studies indicate that large-scale conversion of forest land to farmland will diminish its regulatory and supporting ecosystem services, as forests provide more valuable ecological units than farmland. A study focusing on the temporal changes in ecological value within the Lijiang River Basin from 2020 to 2030 further demonstrated that the conversion of forest land into construction land constitutes the dominant factor leading to the decline of regional ecological value (Li, Wu, Gao, Zheng, Wu, & Li, 2021). In addition, the intensification of tourism activities and the accompanying construction projects will inevitably exert adverse impacts on the structural integrity and functional stability of wetland ecosystems, which in turn weakens the supply capacity of ecosystem services provided by wetlands (You, Ji, Wu, Deng, Huang, Chen, Yu, & He, 2017; Yang et al., 2023).

Although this study reveals the spatiotemporal evolution of land use and landscape patterns in the two heritage sites, given the particularity of karst landforms and the complexity of landscape evolution, the research has achieved a systematic analysis yet still leaves room for further improvement in terms of the universality of the landscape pattern index system and the in-depth analysis of evolution driving mechanisms.

5. Discussion

The results indicated that the overall landscape patterns of the two heritage sites remained stable during the study period, with forest land serving as the core dominant landscape type in both areas, and the evolution characteristics of land use and landscape patterns exhibited significant regional differentiation. Shibing Karst was characterized by the conversion of forest land to cultivated land, with a substantial increase in the area of cultivated land and a continuous reduction in forest land area. The landscape diversity and evenness indices showed a slight increase; the high-value areas of landscape

connectivity, aggregation and other indices were stably distributed in the central part of the heritage site, while the northern and southeastern parts were the high-value areas of landscape shape complexity and diversity indices, and the high-value areas of some indices showed a trend of transforming into low-value areas in the later period. Libo-Huanjiang Karst was featured by a steady growth in forest land area and a significant decrease in shrub land area, with land use conversion concentrated among forest land, cultivated land and shrub land. The landscape connectivity always maintained a high level; the high-value areas of aggregation indices were distributed in the eastern part, and the low-value areas in the central part gradually evolved into medium-value areas after 2010, while the high-value areas of landscape diversity indices were concentrated in the central, western and northern regions. Meanwhile, the construction land in both regions presented a continuous growth trend with a significantly higher dynamic degree than other landscape types, and the water area remained stable overall.

Declaration of Competing Interest

The authors declare that there are no conflicts of interest.

References

Allan, J. R., Venter, O., Maxwell, S., Bertzky, B., Jones, K., Shi, Y., & Watson, J. E. (2017). Recent increases in human pressure and forest loss threaten many natural world heritage sites. *Biological conservation*, *206*, 47-55.

Bai, X., Xiong, K., Chen, Y., & Liu, Z. (2024). Spatiotemporal evolution of landscape stability in world heritage karst sites: a case study of shibing karst and libo-huanjiang karst. *Heritage Science*, *12*, 215.

Chen, S., Tong, Q., & Guo, H. (1998). *Remote sensing information mechanism research*.

Chen, Y., Cheng, C., Xiong, K., Rong, L., & Zhang, S. (2024). Quantifying the biodiversity and ecosystem service outcomes of karst ecological restoration: A meta-analysis of south china karst. *Catena*, *245*, 108278.

Fei, G., Xiong, K., Fei, G., Zhang, H., & Zhang, S. (2023). The conservation and tourism development of world natural heritage sites: The current situation and future prospects of research. *Journal for Nature Conservation*, *72*, 126347.

Ford, D., & Williams, P. D. (2007). *Karst hydrogeology and geomorphology*. John Wiley & Sons.

Fu, B., Wang, S., Su, C., & Forsius, M. (2013). Linking ecosystem processes and ecosystem services. *Current Opinion in Environmental Sustainability*, *5*, 4-10.

Kenterelidou, C., & Galatsopoulou, F. (2021). Sustainable biocultural heritage management and communication: The case of digital narrative for unesco marine world heritage of outstanding universal value. *Sustainability*, *13*, 1449.

Lan, J., Wang, S., Wang, J., Qi, X., Long, Q., & Huang, M. (2022). The shift of soil bacterial community after afforestation influence soil organic carbon and aggregate stability in karst region. *Frontiers in Microbiology*, *13*, 901126.

Li, C., Wu, Y., Gao, B., Zheng, K., Wu, Y., & Li, C. (2021). Multi-scenario simulation of ecosystem service value for optimization of land use in the sichuanyunnan ecological barrier, china. *Ecological Indicators*, *132*, 108328.

Liu, Q., Wang, J., Xiong, K., Gong, L., Chen, Y., Yang, J., Xiao, H., & Bai, J. (2024). Quantitative assessment of ecological assets in the world heritage karst sites based on remote sensing: With a special reference to south china karst. *Heritage Science*, *12*.

Liu, Y., Hou, X., Li, X., Song, B., & Wang, C. (2020). Assessing and predicting changes in ecosystem service values based on land use/cover change in the bohai rim coastal zone. *Ecological Indicators*, *111*, 106004.

Luo, L., Wang, H., Chen, Z., Wang, X., & Guo, H. (2024). Biodiversity cobenefits of world heritage protection. *The Innovation Life*, *2*, 100051.

Osipova, E., Shadie, P., Zwahlen, C., Osti, M., Shi, Y., Kormos, C., Bertzky, B., Murai, M., Van Merm, R., & Badman, T. (2017). *Iucn world heritage outlook 2: A conservation assessment of all natural world heritage sites*. (No Title) .

Su, S., Xiao, R., Jiang, Z., & Zhang, Y. (2012). Characterizing landscape pattern and ecosystem service value changes for urbanization impacts at an ecoregional scale. *Applied Geography*, *34*, 295-305.

Sweeting, M. M. (1986). Limestone landscapes of south china. *Geology today*, *2*, 11-16.

Tarr, N. M. (2019). Demonstrating a conceptual model for multispecies landscape pattern indices in landscape conservation. *Landscape Ecology*, *34*, 2133-2147.

Tian, S. (2008). *Study on formation and evolution of cone karst landforms in lipu world natural heritage site*. Guizhou Normal University .

Turner, M. G. (2005). Landscape ecology: what is the state of the science? *Annu. Rev. Ecol. Evol. Syst*, *36*, 319-344.

Wang, Y., Dai, E., Ge, Q., Zhang, X., & Yu, C. (2021). Spatial heterogeneity of ecosystem services and their trade-offs in the hengduan mountain region, southwest china. *Catena*, *207*, 105632.

Xiong, K. (1990). Karst landscape and environmental conservation in new zealand. *Journal of Guizhou Normal University*, *13*, 16-25.

Xiong, K., Chen, D., Zhang, J., Gu, X., & Zhang, N. (2023). Synergy and regulation of the south china karst wh site integrity protection and the buffer zone agroforestry development. *Heritage Science*, *11*, 218.

Xiong, K., Li, G., & Wang, L. (2012). Study on the protection and sustainable development of south china karst libo world natural heritage site. *Chin Gard*, *28*, 66-71.

Yan, X., & Li, L. (2023). Spatiotemporal characteristics and influencing factors of ecosystem services in central asia. *Journal of Arid Land*, *15*, 1-19.

Yang, J., Zhai, D.L., Fang, Z., Alatalo, J.M., Yao, Z., Yang, W., Su, Y., Bai, Y., Zhao, G., & Xu, J. (2023). Changes in and driving forces of ecosystem services in tropical southwestern china. *Ecological Indicators*, *149*, 110180.

Yang, M. (1990). The vulnerability of karst environment. *Yunnan Geographical Environment Research*, *2*, 21-29.

You, W., Ji, Z., Wu, L., Deng, X., Huang, D., Chen, B., Yu, J., & He, D. (2017). Modeling changes in land use patterns and ecosystem services to explore a potential solution for meeting the management needs of a heritage site at the landscape level. *Ecological Indicators*, *73*, 68-78.

Yuan, D. (1992). Karst in southwest china and its comparison with karst in north china. *Quaternary Sciences*, *12*, 352-361.

Zeng, C., He, J., He, Q., Mao, Y., & Yu, B. (2022). Assessment of land use pattern and landscape ecological risk in the chengdu-chongqing economic circle, southwestern china. *Land*, *11*, 659.

Zeng, X., Huang, Y., Xie, H., Ma, Q., & Li, J. (2024). Impacts of land use and land cover change on the landscape pattern and ecosystem services in the poyang lake basin, china. *Landscape Ecology*, *39*, 183.

Zhang, Y. (2025). *Strategies for ecosystem vulnerability adjustment and resilience enhancement in karst world heritage sites*. Guizhou Normal University.